URSI AP-RASC 2019, New Delhi, India; 09 - 15 March 2019

Millimeter-Wave Quad-Port Multiple-Input Multiple-Output Dielectric Resonator Antenna Excited Differentially by TE_{20} Mode Substrate Integrated Waveguide

Abhishek Sharma(1), Anirban Sarkar(1), Animesh Biswas(1) and M. Jaleel Akhtar(1)
(1) Department of Electrical Engineering, Indian Institute of Technology Kanpur, Kanpur-208016, UP, India

Abstract

In this paper, a differentially excited quad-element multiple-input multiple-output (MIMO) dielectric resonator antenna (DRA) is proposed for millimeter-wave applications. In the proposed design, the rectangular DRA is differentially excited in the $TE^{y}_{1\delta1}$ mode using the dual-slot configuration located on the top wall of TE_{20} mode substrate integrated waveguide (SIW). The proposed MIMO configuration offers both spatial and polarization diversities. For all the four ports, the impedance bandwidth of the proposed antenna is 3.2% (27.5-28.4 GHz), covering the 5G frequency spectrum. The isolation between the input ports is better than 40 dB throughout the operating bandwidth. The antenna radiates along the broadside direction having the cross-polarization level below -30 along the zenith. The peak gain and radiation efficiency of the proposed antenna is 4.2 dBi and 86%, respectively at 28 GHz. Moreover, the diversity performance is found to be good having low value of envelope correlation coefficient across the bandwidth. The proposed antenna could be the potential candidate for next generation 5G communication system.

1 Introduction

With the colossal growth of the wireless communication system, there is prodigious demand for superior data rate, better reliability, robustness, and lower latency. With regard to this, the multiple-input multiple-output (MIMO) technology has emerged as a new paradigm and significantly changed the wireless communication systems in the recent past [1]. The MIMO system utilizes multiple antennas at both the transmitting and receiving ends which significantly increases the data rates and link reliability. Nowadays, for the modern wireless communication system, the need of signal integrity is more extensive than ever. To achieve higher signal-to-noise (SNR) ratio, differential-signalling technique can be employed which can suppress the common-mode interference and consequentially enhances the signal quality [2]. The differential feeding can also be effective in suppressing cross-polarized fields and can directly be integrated with the differential circuits. This leads to the introduction of differential antennas and several planar differential antennas and differentially-fed MIMO antennas have been proposed in the past [3–5].

As a matter of fact, the inherent advantages of the DRA such as small size, low loss, relatively wider bandwidth, high efficiency (due to negligible conductor loss and no surface wave generation), ease of excitation makes it more preferable over the conventional microstrip antennas [6]. However, relatively limited literature is available for differentially-fed DRAs and differentially-fed diversity DRAs [2, 7–11]. The first differentially-fed DRA has been investigated in [2] in which a rectangular DRA was excited in TE_{111} mode at 2.4 GHz. Here, the authors have utilized commercially available 180° hybrid coupler which undesirably increases the system size. To overcome this, the authors in [7] have proposed a hollow DRA with an underlaid rat-race coupler for the differential feeding through the two conformal strip. A broadband singly fed differential DRA with high boresight gain has been investigated in [8], where a pair of microstrip lines has been used for excitation of the DRA. More recently, a differentially fed DRA and 2×2 array with parallel feeding structure has been proposed in [9] which exhibits an impedance bandwidth of 22% with the balun. In [10], a differential dual-band dual-polarized DRA with high isolation and low cross polarization has been proposed using the cross-shaped DRA.

All the above mentioned differentially-driven DRAs have been designed in the lower frequency band and were exited either by co-axial probe or microstrips (MS). However, the feeding through probe or MS can cause the undesirable radiation leakage and losses at the millimeter wave frequency. To minimize these losses, the transmission line with low-loss such as rectangular waveguide, gap waveguide, etc. can be employed but the non-planar nature limits their use with monolithic microwave integrated circuit (MMIC) technology and low profile applications. To alleviate this limitation, the substrate integrated waveguide (SIW) technology has emerged as a promising candidate and widely adopted for mm-wave applications [12–14]. In this paper, a differentially excited rectangular DRA has been proposed for 5G communication system. The proposed antenna element is then used to realize four port MIMO system offering both spatial and polarization diversities. The rectangular DRA is excited in the $TE^{y}_{1\delta1}$ mode by the dual-slot configuration located in the top wall of SIW operating in TE_{20} mode. The intrinsic electric field

distribution of TE_{20} mode SIW helps to excite the DRA differentially using the dual-slot.

2 Antenna Design

Figure 1 shows the electric field distribution of TE_{20} mode in the SIW structure. From the figure it is observed that with respect to the center line AB, the electric field shows the odd symmetry *i.e.* the electric field has the same amplitude but reversed phase along the line of symmetry. Therefore, this characteristics of TE_{20} mode allows the

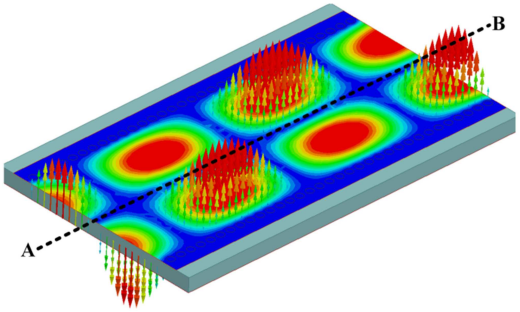

Figure 1. TE_{20} mode electric field distribution in substrate integrated waveguide.

differential excitation of rectangular DRA using dual-slot located at the top wall of SIW. In order to efficiently excite the TE_{20} mode, one can use the two coplanar microstrip-to-waveguide transitions that can generate two out-of-phase field vectors at the waveguide input [15]. The SIW is designed on Rogers RT/Duroid 5880 of relative permittivity 2.2 and thickness 0.787 mm.

Figure 2 shows the proposed differentially excited rectangular DRA and its quad-element MIMO configuration. The material used to design the DRA is Rogers RT/Duroid 6010 of relative permittivity 10.2 and height 1.5 mm. The lateral dimensions of the DRA are: $A = 2.8$ mm, $B = 3.4$ mm. The energy to the DRA is coupled through the two narrow apertures situated on the top wall of SIW. The electric field distribution depicted in Figure 3 confirms the excitation of $TE^{y}_{1\delta 1}$ mode in the rectangular DRA using the dual-slot configuration.

3 Results and Discussions

3.1 Impedance and Radiation Performance

The simulated response of the proposed quad-element MIMO DRA is shown in Figure 4. The antenna elements (DR1, DR3) and (DR2, DR4) provide spatial diversity whereas the orthogonal placement of the adjacent elements (for eg. DR1, DR2) offer polarization diversity. The theoretical resonant frequency for the DRA is 25.2 GHz whereas the corresponding simulated value is 28 GHz. This discrepancy is due to the fact that in the theoretical analysis the infinite ground plane was considered and the

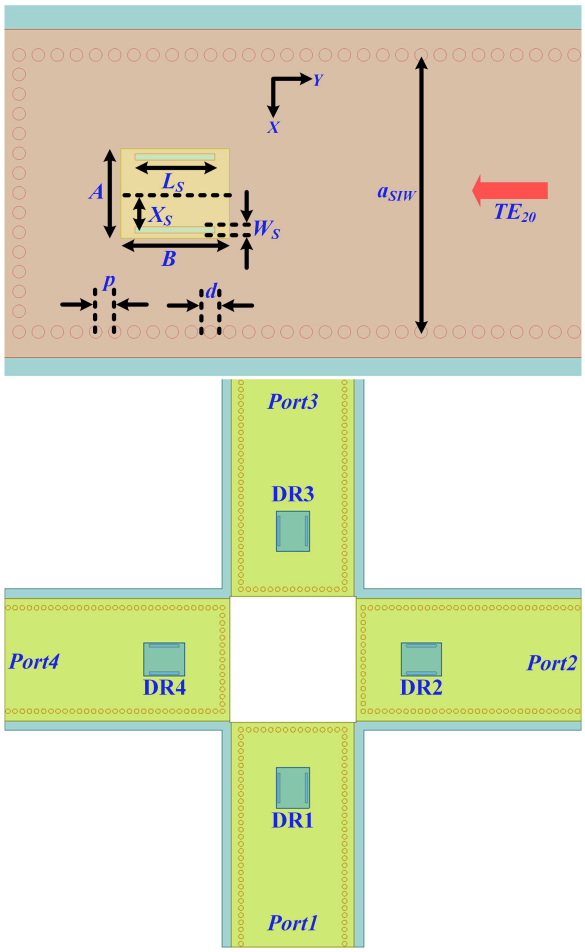

Figure 2. Schematic of proposed SIW fed DRA (a) Single element (b) MIMO. Geometrical Parameters: $p = 0.6$, $d = 0.4$, $a_{SIW} = 8.7$, $L = 3.4$, $W = 2.8$, $L_S = 2.5$, $W_S = 0.2$, $X_S = 1.05$ (all dimensions are in mm).

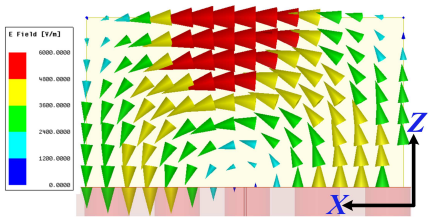

Figure 3. Electric field distribution at 28 GHz in (a) SIW (b) DRA.

effect of slot was also not taken into account. Similar kind of discrepancy has also been observed in [12].

For all the four ports, the simulated impedance bandwidth of the proposed antenna is 3.2% (27.5-28.4 GHz), covering the 5G frequency spectrum provided by federal communication commission (FCC) [16]. From the figure 4, it is observed that the isolation between the input ports is better than 40 dB through out the bandwidth.

Figure 5 shows the 3D radiation pattern of the pro-

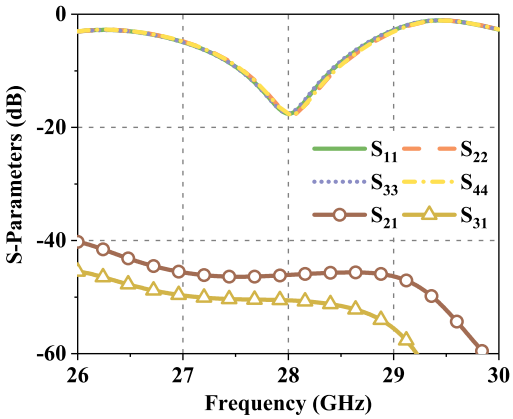

Figure 4. S-Parameters of the proposed MIMO antenna.

posed MIMO antenna at 28 GHz for *Port1* to *Port4*. From the figure, it is observed that there is a change of polarization with the change of feeding port without any variation in the radiation pattern, confirming the diversity nature. Figure 6(a) shows the radiation pattern of the single isolated element (refer Figure 2(a)). The antenna radiates along the broadside direction with the cross-polarized level below -25 dB in XZ-plane and -30 dB in YZ-plane. Figure

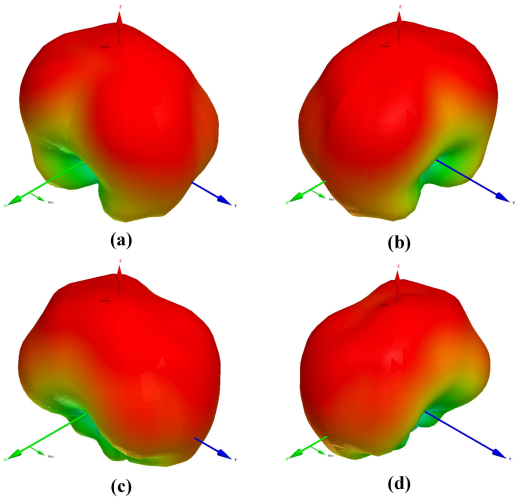

Figure 5. 3D radiation pattern at (a) *Port1* (b) *Port2* (c) *Port3* (d) *Port4*.

6(b) depicts the radiation pattern of the antenna element DR1 with *Port2* to *Port4* terminated into the matched load. The antenna element DR1 radiates along the zenith and the difference between the co-polarized and the cross-polarized field is >30 dB along the zenith in both the planes. The simulated peak gain and radiation efficiency of the MIMO antenna at 28 GHz is 4.2 dBi and 86%, respectively.

3.2 Diversity Performance

The envelope correlation coefficient (ECC) is an important parameter which is usually determined using the far field pattern of the multi antenna system. Considering the sim-

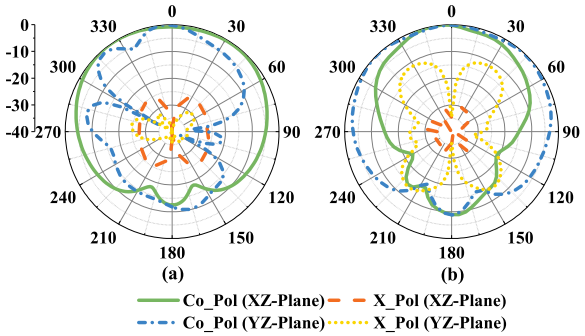

Figure 6. 2D radiation pattern at 28 GHz (a) Single element (b) Antenna element DR1.

Table 1. Envelope Correlation Coefficient

Frequency (GHz)	$\rho_{e,12}$	$\rho_{e,13}$
27.5	0.0001	0.0001
27.7	0.00006	0.0002
27.9	0.00002	0.0003
28.1	0.00002	0.0002
28.3	0.00003	0.0002
28.5	0.00004	0.0002

plest case *i.e.*, the uniform/isotropic propagation scenario, the ECC can be determined as:

$$\rho_{e,ij} = \frac{\left|\int_{4\pi}\left(\vec{E}_i(\theta,\phi) * \vec{E}_j(\theta,\phi)\right) d\Omega\right|^2}{\int_{4\pi}\left|\vec{E}_i(\theta,\phi)\right|^2 d\Omega \int_{4\pi}\left|\vec{E}_j(\theta,\phi)\right|^2 d\Omega}, \quad (1)$$

where, $E_i(\theta,\phi)$ is the complex 3D radiated field pattern of the i^{th} antenna element, Ω denotes the solid angle and $*$ represents the complex conjugate operator. The values of ECC across the operating bandwidth is tabulated in Table 1. The values of ECC for the proposed antenna are well below the standard limit (ECC<0.5), indicating effective diversity performance.

To characterize the bandwidth and radiation performance of the multi-port antenna, total active reflection coefficient (TARC) is evaluated. It accounts the mutual coupling between the elements and random-signal combinations between the input ports. TARC for N port antenna system can be evaluated as:

$$\Gamma_a^t = \sqrt{\frac{\sum_{i=1}^{N}|b_i|^2}{\sum_{i=1}^{N}|a_i|^2}} \quad (2)$$

where a_i is the incident signal, b_i is the reflected signal and $\mathbf{b} = [S]\mathbf{a}$. From the figure 7, it is observed that TARC $<$ -10 dB and the curve retain the original characteristics of the single antenna with slight change in the operating frequency and bandwidth.

4 Conclusion

In this paper, a rectangular DRA excited by dual-slot situated on the top wall of TE_{20} mode SIW has been presented

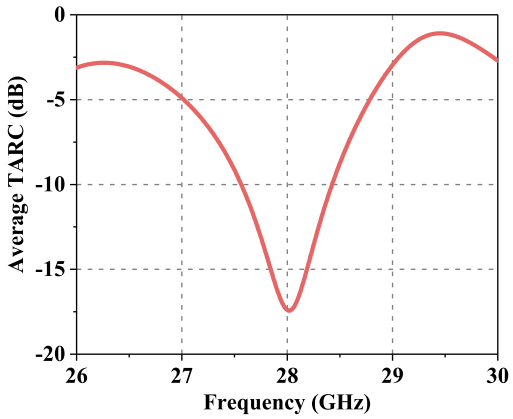

Figure 7. Average TARC of the proposed MIMO system.

for next generation 5G communication system. The intrinsic field distribution of TE_{20} mode SIW excites the rectangular DRA differentially in the fundamental $TE^{y}_{1\delta 1}$ using the dual-slot configuration. The single element has been utilize to implement quad-element MIMO system offering both spatial and polarization diversities. The proposed antenna exhibits an impedance bandwidth of 3.2% (27.5-28.4 GHz) for all the four ports and the port-to-port isolation of better than 40 dB has been achieved across the bandwidth. The antenna radiates along the broadside direction having the cross polarization level better than -30 dB along the zenith in both the planes. The peak gain and radiation efficiency of 4.2 dBi and 86% has been achieved at 28 GHz. Furthermore, the diversity performance of the proposed antenna has been found to be good with ECC well below 0.5 and TARC $<$ -10 dB.

References

[1] M. S. Sharawi, "*Printed MIMO Antenna Engineering*," Artech House, 2014.

[2] Bin Li, and K. W. Leung, "On the differentially fed rectangular dielectric resonator antennas," *IEEE Transactions on Antennas and Propagation*, **56**, 2, 2008, pp. 353–359.

[3] J. Y. Siddiqui, S. Datta, M. Caillet, and Y. M. M. Antar, "Compact differentially fed inverted microstrip circular patch with an integrated coupler," *IEEE Antennas and Wireless Propagation Letters*, **9**, 2010, pp. 627–630.

[4] Y. Liu, Z. Tu and Q. Chu, "Differentially T-shape slot antenna with high common-mode suppression for 2.4/5.2/5.8 GHz WLAN MIMO systems," in *2015 Asia-Pacific Microwave Conference (APMC)*, Nanjing, 2015.

[5] Y. Sharma, D. Sarkar, K. Saurav and K. V. Srivastava, "Differential quasi self-complimentary (QSC) ultra-wideband (UWB) MIMO antenna," in *2017 IEEE International Conference on Antenna Innovations & Modern Technologies for Ground, Aircraft and Satellite Applications (iAIM)*, Bangalore, 2017, pp. 1-4.

[6] A. Petosa, "*Dielectric Resonator Antenna Handbook*," Artech House, 2007.

[7] X. S. Fang, K. W. Leung, E. H. Lim, and R. S. Chen, "Compact differential rectangular dielectric resonator antenna," *IEEE Antennas and Wireless Propagation Letters*, **9**, 2010, pp. 662–665.

[8] R. D. Gupta, and M. S. Parihar, "Differentially fed wideband rectangular DRA with high gain using short horn," *IEEE Antennas and Wireless Propagation Letters*, **16**, 2017, pp. 1804–1807.

[9] Sheng-Jie Guo, Lin-Sheng Wu, Kwok Wa Leung, and Jun-Fa Mao, "Microstrip-fed differential dielectric resonator antenna and array," *IEEE Antennas and Wireless Propagation Letters*, **17**, 2018, pp. 1736–1739.

[10] H. Tang, Jian-Xin Chen, Wen-Wen Yang, Li-Heng Zhou, and W. Li, "Differential dual-band dual-polarized dielectric resonator antenna," *IEEE Transactions on Antennas and Propagation*, **65**, 2, 2017, pp. 855–860.

[11] A. Sharma, A. Sarkar, M. Adhikary, A. Biswas, M. J. Akhtar, "Equilateral triangular dielectric resonator based co-radiator MIMO antennas with dual polarisation," *IET Microwaves, Antennas and Propagation*, 2018, DOI: 10.1049/iet-map.2018.5035.

[12] W. M. A. Wahab, D. Busuioc, and S. Safavi-Naeini, "Low cost planar waveguide technology-based dielectric resonator antenna (dra) for millimeter-wave applications: analysis, design, and fabrication," *IEEE Transactions on Antennas and Propagation*, **58**, 8, pp. 2499–2507, 2010.

[13] A. Sharma, A. Sarkar, M. Adhikary, A. Biswas, M. J. Akhtar, "SIW fed MIMO DRA for future 5G applications," in *2017 IEEE International Symposium on Antennas and Propagation and USNC-URSI Radio Science Meeting*, San Diego, 2017.

[14] H. Jin, W. Che, K. S. Chin, W. Yang, and Q. Xue, "Millimeter-Wave TE_{20} mode SIW dual-slot-fed patch antenna array with a compact differential feeding network," *IEEE Transactions on Antennas and Propagation*, **66**, 1, 2018, pp. 456-461.

[15] Asanee Suntives, and Ramesh Abhari, "Design and application of multimode substrate integrated waveguides in parallel multichannel signaling systems," *IEEE Transactions on Antennas and Propagation*, **57**, 6, 2009, pp. 1563–1571.

[16] W. Hong, Z. H. Jiang, C. Yu, *et al.*, "Multibeam antenna technologies for 5G wireless communications," *IEEE Transactions on Antennas and Propagation*, **65**, 12, pp. 6231–6249, 2017.